Huntingtin-interacting Protein 1 Promotes Vpr-induced G2 Arrest and HIV-1 Infection in Macrophages

Tomoyuki Murakami
RIKEN: Rikagaku Kenkyujo
Nopporn Chutiwitoonchai
RIKEN: Rikagaku Kenkyujo
Masami Takei
Nihon University School of Medicine Graduate School of Medicine: Nihon Daigaku Igakubu Daigakuin Igaku Kenkyuka
Yoko Aida (aida@riken.jp)
Baton Zone Program, RIKEN Cluster for Science, Technology and Innovation Hub, 2-1 Hirosawa, Wako, Saitama 351-0198, Japan 351-0198, Japan https://orcid.org/0000-0001-7400-3587

Research

Keywords: HIV-1, Vpr, G2 arrest, siRNA, CELAVIEW RS100, flow cytometry, HIP1, macrophage

DOI: https://doi.org/10.21203/rs.3.rs-76686/v1

Abstract

Background: Human immunodeficiency virus type 1 (HIV-1) modulates the host cell cycle. The HIV-1 accessory protein Vpr arrests the cell cycle at G2 phase, which is important for efficient viral replication in dividing $CD4^+$ T cells, because the transcriptional activity of the HIV-1 long terminal repeat is most active in G2 phase. Additionally, Vpr-mediated G2 arrest likely correlates with enhanced HIV-1 infection in monocyte-derived macrophages.

Results: Here, we screened small-interfering RNA to reveal candidates that suppress Vpr-induced G2 arrest and identified Huntingtin-interacting protein 1 (HIP1) as both directly interacting with Vpr and required for efficient G2 arrest. Interestingly, HIP1 was not essential for Vpr-induced DNA double-strand breaks, which are required for activation of the DNA-damage checkpoint and G2 arrest. Furthermore, *HIP1* knockdown suppressed HIV-1 infection in monocyte-derived macrophages.

Conclusions: These results suggest that HIP1 operates in the downstream step(s) of DNA-damage induction to promote Vpr-induced G2 arrest and enhances HIV-1 infection in macrophages.

Background

Vpr is an accessory gene product of human immunodeficiency virus type 1 (HIV-1) and a small 15-kDa protein with multiple biological functions, including splicing regulation [1–3], support of virus release [4], nuclear import of the viral preintegration complex in macrophages [5–7], enhanced expression and processing of the envelope glycoprotein in macrophages [8–10], sustaining interleukin 6 expression to enhance HIV-1 replication [11], antagonism of exonuclease 1- and helicase-like transcription factor-mediated restriction in T cells through degradation of these proteins [12–15], regulation of apoptosis in both a positive and negative manner, and induction of cell cycle arrest at G2 phase in dividing cells [16–21]. Multiple functions of Vpr are exerted through interactions with various host factors, such as DNA damage-binding protein 1 (DDB1)- and cullin 4 (CUL4)-associated factor 1 (DCAF1), spliceosome-associated protein 145, p300, synthetic lethal of unknown (X) function 4 (SLX4), protein arginine N-methyltransferase 5, importin α, and mini-chromosome maintenance protein10 [1, 5, 6, 12, 20, 22–26]. Induction of G2 arrest is likely an important function for efficient viral replication because the transcriptional activity of the HIV-1 long terminal repeat (LTR) is most active in the G2 phase [27, 28]. Indeed, the ability of Vpr to cause cell cycle blockade is well conserved among primate lentiviruses [29, 30]. Additionally, Vpr accelerates acute HIV-1 infection by exploiting proliferating $CD4^+$ T cells, including regulatory $CD4^+$ T cells, through G2 arrest and apoptosis *in vivo* [31].

Moreover, Vpr induces DNA damage and activates ataxia telangiectasia-mutated and Rad3-related protein (ATR) to induce G2 arrest [32–34]. Vpr-induced G2 arrest requires the association of Vpr with the CUL4 ubiquitin ligase in association with DDB1 and DCAF1 [23, 35–39]. Although previous reports indicate that interaction between CUL4–Vpr and the SLX4 complex is necessary for efficient induction of

G2 arrest [24, 40], Fregoso et al. [41] demonstrated that Vpr induces G2 arrest independent of SLX4. Thus, the full molecular mechanism(s) underlying Vpr-induced G2 arrest remain unknown.

Macrophages are a cellular target of HIV-1. In HIV-1-infected patients, macrophages reportedly act as a viral reservoir widely distributed throughout multiple tissues under the combination antiretroviral therapy [42, 43]. Vpr enhances HIV-1 infection in macrophages through various mechanisms [5–11, 44], and a Vpr mutant showing defective induction of G2 arrest also fails to promote HIV-1 infection in macrophages [44]. Therefore, it is possible that Vpr-mediated G2 arrest is implicated in efficient HIV-1 infection in macrophages, and that understanding of Vpr-specific G2-arrest mechanism(s) could reveal how Vpr facilitates HIV-1 infection in macrophages.

Huntingtin-interacting protein 1 (HIP1) interacts with the protein encoded by the gene mutated in Huntington's disease [45, 46], an inherited neurodegenerative disorder caused by expansion of the codon CAG in the *Huntingtin* gene and resulting in translation of a polyglutamine tract in the protein. The affinity of the Huntingtin–HIP1 interaction is inversely correlated with the polyglutamine-repeat length [45, 46]. Additionally, HIP1 is associated not only with Huntingtin's disease but also various cellular processes, including clathrin-mediated endocytosis [47–49], tumorigenesis [50, 51], and neuronal cell death [52, 53].

In this study, we investigated the novel molecular mechanism of Vpr-mediated G2 arrest by screening candidate(s) directly involved in this process through the use of a small-interfering (si)RNA mini-library of target genes and CELAVIEW RS100, an imaging-based screening microscope. CELAVIEW RS100 automatically acquires cellular fluorescence images and quantitatively analyzes the morphology and fluorescence signal in a large number of cells. Compared with flow cytometry analysis, CELAVIEW RS100 enables high-throughput analysis of DNA contents in the Hoechst33342-stained nuclei of large numbers of Vpr-expressing cells. As a second screening, we determined whether the candidate(s) were truly involved in Vpr-induced G2 arrest using flow cytometry analysis. Screening results identified HIP1 as a novel host factor involved in Vpr-induced G2 arrest, after which we examined the effect of *HIP1* knockdown on HIV-1 infection in macrophages.

Results

HIP1 enhances Vpr-induced G2 arrest

To identify new cellular factor(s) involved in Vpr-induced G2 arrest, we used CELAVIEW RS100 for the initial screening in combination with an siRNA mini-library containing 256 siRNAs. CELAVIEW RS100 enables high-throughput analysis of DNA contents via automated image acquisition and data analysis. As shown in Fig. 1A, HeLa cells were transfected with a bicistronic vector [pME18Neo/Flag-Vpr-internal ribosomal entry site (IRES)-ZsGreen1] encoding Flag tagged-wild-type (WT) Vpr (Flag-Vpr) and ZsGreen1 as a marker of Vpr expression, together with the siRNAs. At 48-h post-transfection, the cells were fixed and stained with Hoechst33342 for analysis of DNA contents using CELAVIEW RS100. Among the 256 siRNAs, 36 inhibited Vpr-induced G2 arrest in ZsGreen1+ cells, with data indicating HIP1 as a critical model (Fig. 1A).

To confirm the screening results, we performed secondary screening to investigate the effect of these siRNAs on cell cycle progression in HeLa cells using flow cytometry analysis. Among the 36 siRNAs, that targeting *HIP1*, which is predominantly expressed in the brain and interacts with Huntingtin [45, 46], inhibited Vpr-induced G2 arrest (Fig. 1B).

To verify whether *HIP1* knockdown impairs Vpr-induced G2 arrest, we designed two other siRNAs targeting different *HIP1*-encoded sequences (#1 and #2). Western blotting subsequently confirmed knockdown of HIP1 levels in HeLa cells transfected with either pME18Neo/Flag-IRES-ZsGreen1 or pME18Neo/Flag-Vpr-IRES-ZsGreen1 together with either #1 or #2 siRNA (Fig. 2A). At 48-h post-transfection of HeLa cells with either pME18Neo/Flag-IRES-ZsGreen1 or pME18Neo/Flag-Vpr-IRES-ZsGreen1 and each respective siRNA, we determined the cell cycle distribution of the ZsGreen1+ cells using CELAVIEW RS100. Knockdown of HIP1 levels did not affect cell cycle progression in cells transfected with pME18Neo/Flag-IRES-ZsGreen1 and either siRNA (Fig. 2B). Additionally, we identified a dose-dependent decrease in Vpr-induced G2 arrest in HeLa cells transfected with either *HIP1* siRNA, resulting in inhibition levels up to ~40% and 45% for #1 and #2, respectively, which were not observed in cells transfected with negative control siRNA (Fig. 2B). Furthermore, this reduction in G2 arrest was restored by up to ~40% by overexpression of siRNA-resistant *HIP1* (siR-HIP1), which carries synonymous nucleotide mutations in the third codons of the siRNA-targeted sequence (Fig. 2C). These results suggested that HIP1 augments Vpr-induced G2 arrest.

We then determined whether G2 arrest induced by etoposide, which is an inhibitor of DNA topoisomerase II and inducer of DNA damage, is inhibited by *HIP1* knockdown (siRNA #2) in HeLa cells. CELAVIEW RS100 results showed that etoposide-induced G2 arrest was not inhibited by *HIP1* knockdown (Fig. 2D and E), implying that HIP1 exerts a specific action on Vpr-induced G2 arrest.

HIP1 directly interacts with Vpr

To investigate whether HIP1 interacts with Vpr, we used a glutathione-S-transferase (GST) pull-down assay. Incubation of recombinant GST-tagged Vpr (GST-Vpr; immobilized on glutathione-Sepharose beads) with HA-tagged HIP1 protein (HA-HIP1) purified from 293T cells transfected with pCAGGS/HA-HIP1, followed by GST pull-down assay, clearly revealed that HIP1 directly bound Vpr (Fig. 3A). To confirm the interaction between HIP1 and Vpr in cells, we performed immunoprecipitation assays using lysate from 293T cells transfected with pME18Neo/Flag-Vpr together with pCAGGS/HA-HIP1, which revealed a HIP1–Vpr interaction (Fig. 3B). These results suggested that Vpr possibly induces G2 arrest via direct interactions with HIP1.

HIP1 is dispensable for Vpr-induced DNA double-strand breaks

Vpr induces DNA double-strand breaks and G2 arrest via interactions with the CUL4 ubiquitin ligase in association with DDB1 and DCAF1 [23, 35-39, 54]. Because HIP1 binds Vpr, we hypothesized that HIP1 cooperates with CUL4 to promote Vpr-induced DNA damage. To test the hypothesis, we analyzed the effect of *HIP1* knockdown on Vpr-induced formation of DNA-repair foci containing phosphorylated

histone 2A variant X (γ-H2AX), which forms distinct nuclear foci following Vpr-induced DNA double-strand breaks [33]. After transfection with pME/Flag-Vpr-IRES-ZsGreen1 together with *HIP1* siRNA #2 and/or *DCAF1* siRNA (as a positive control siRNA for inhibition of Vpr-induced DNA double-strand breaks [54]), we performed immunofluorescence staining and confocal microscopy analysis to detect γ-H2AX foci and investigated cell cycle status using CELAVIEW RS100. Fig. 4A shows western blot confirmation of decreased HIP1 and DCAF1 levels. Interestingly, although HIP1 knockdown alone diminished G2 arrest (Fig. 4C), this did not suppress Vpr-induced formation of γ-H2AX foci (Fig. 4B). By contrast, knockdown of DCAF1 alone or both HIP1 and DCAF1 completely inhibited both Vpr-induced formation of γ-H2AX foci (Fig. 4B) and G2 arrest (Fig. 4C). These results indicated that HIP1 is dispensable for Vpr-induced DNA double-strand breaks, and that HIP1 possibly plays a role in Vpr-induced G2 arrest independent of DCAF1.

HIP1 promotes HIV-1 infection in macrophages

In primary macrophages, Vpr enhances HIV-1 infection, whereas a Vpr mutant that is unable to induce G2 arrest does not enhance HIV-1 infection in macrophages [44]. Therefore, it is possible that HIP1 also contributes to efficient HIV-1 infection in macrophages. To investigate whether HIP1 is involved in enhancing Vpr-mediated HIV-1 infection in primary macrophages, monocyte-derived macrophages were differentiated from monocytes isolated from human peripheral blood mononuclear cells (PBMCs), as described previously [6, 26]. These macrophages were then transfected with *HIP1* siRNA#2 and then infected with the vesicular stomatitis virus G protein (VSV-G)-pseudotyped NL4-3-Luc HIV-1 encoding either WT Vpr (Vpr+ virus) or truncated Vpr (Vpr^- virus), which can only support a single round of HIV-1 replication, at 24-h post-transfection. Following confirmation of attenuated HIP1 levels by western blotting (Fig. 5A), we determined infectivity by measuring luciferase activity at 6-days post-infection. The luciferase activity in both Vpr+ and Vpr^- cells was reduced by *HIP1* knockdown, with the reduction in Vpr+ cells slightly larger than that in Vpr^- cells (~43% in Vpr+ cells *vs.* ~33% in Vpr^- cells) (Fig. 5B). These results suggested that although HIP1 contributes to HIV-1 infection in macrophages, it likely promotes stronger infection-related activity via cooperation with Vpr.

Discussion

Various factors are required for Vpr-induced G2 arrest, including activation of the ATR pathway and interaction with CUL4 ubiquitin ligase in association with DDB1 and DCAF1 [23, 24, 32–35, 37–39, 55]. In the present study, siRNA screening identified HIP1 as a new host factor that modulates not only Vpr-induced G2 arrest but also HIV-1 infection in macrophages. We found that HIP1 enhances Vpr-induced G2 arrest but is not required for Vpr-induced DNA double-strand breaks. Additionally, we revealed that HIP1 contributes to efficient HIV-1 infection in macrophages.

Notably, we demonstrated that HIP1 is not necessary for Vpr-induced DNA double strand breaks. Li et al. [56] reported that although protein phosphatase 2 (PP2A) is important for Vpr-induced G2 arrest, Vpr-induced DNA double-strand breaks is not inhibited by *PP2A* knockdown. Thus, HIP1 possibly collaborates with PP2A to enhance Vpr-induced G2 arrest that is independent of DNA-damage induction.

Vpr induces DNA double-strand breaks and facilitates HIV-1 infection in primary macrophages via associations between Vpr and CUL4 [8, 10, 11, 54]. In the present study, we showed that HIP1 is not involved in Vpr-induced DNA double-strand breaks, and that compared with Vpr-deleted HIV-1, *HIP1* knockdown effectively inhibited WT HIV-1 infection in macrophages. These results suggested that HIP1 is not a component of the CUL4 ubiquitin-ligase complex, and that HIV-1 replication in macrophages is enhanced by HIP1 interaction with Vpr via unknown mechanism(s).

In summary, we showed that HIP1 augments Vpr-induced G2 arrest and HIV-1 infection in macrophages. Although HIP1 binds Vpr, it remains unclear whether this activity is necessary for Vpr-induced G2 arrest. Additionally, although we found that HIP1 efficiently enhanced WT HIV-1 infection in macrophages relative to that by Vpr-deleted HIV-1, the associated mechanism(s) remain to be elucidated. Future investigations are required to determine the exact roles of HIP1 in Vpr-induced G2 arrest and HIV-1 infection in macrophages, as well as provide insights into correlations between the two functions of Vpr.

Conclusions

In this study, we identified HIP1 as a novel host protein that enhances Vpr-induced G2 arrest but is not essential for Vpr-induced DNA damage. Moreover, we showed that HIP1 facilitates HIV-1 infection in primary monocyte-derived macrophages. Because the transcription of HIV-1 LTR is most active in the G2 phase and Vpr accelerates acute infection of HIV-1 *in vivo* through G2 arrest, HIP1 might represent a viable candidate as a novel anti-HIV-1 target to suppress HIV-1 infection in both $CD4^+$ T cells and macrophages.

Methods

Cell culture and transfection

HeLa cells and 293T cells were grown in Dulbecco's modified Eagle's medium (GIBCO, Gaithersburg, MD, USA) supplemented with 10% heat-inactivated fetal bovine serum (FCS; Sigma-Aldrich, St. Louis, MO, USA). Human PBMCs were isolated on a Ficoll (Lymphosepal; Immuno-Biological Laboratories, Minneapolis, MN, USA) gradient from a healthy donor. Monocytes were selected from PBMCs using CD14 MicroBeads (Miltenyi Biotec, Bergisch Gladbach, Germany) and a MACS separation column (Miltenyi Biotec) with a Quandro MACS separation unit (Miltenyi Biotec) according to manufacturer instructions. Monocytes were cultured at the desired density in 6- or 24-well plates and grown in Roswell Park Memorial Institute (RPMI)-1640 medium (Invitrogen, Carlsbad, CA, USA) containing 10% heat-inactivated FCS (Culture Biosciences, San Francisco, CA, USA), 5% AB serum (Sigma-Aldrich), and 10 ng/ml macrophage colony-stimulating factor (M-CSF; PeproTech, Rocky Hill, NJ, USA) for 1 week until they spontaneously differentiated into mature macrophages.

Plasmid transfection was performed using FuGENE HD (Promega, Madison, WI, USA) or Lipofectamine2000 (Invitrogen). siRNA transfection was performed using Lipofectamine2000 or

Lipofectamine RNAi MAX (Invitrogen). siRNA and plasmid co-transfection was performed using Lipofectamine2000. siRNA transfection for macrophages was performed using Lipofectamine RNAi MAX. Macrophages were transfected with 50 nM siRNA in Opti-MEM (GIBCO). At 4-h post-transfection, macrophages were washed and cultured in RPMI-1640 medium containing 10% heat-inactivated FCS, 5% AB serum, and 10 ng/ml M-CSF for 20 h. Cells were subjected to subsequent rounds of transfection, washing, and culturing as described.

Plasmid construction

The expression vector pME18Neo encoding Flag-tagged WT Vpr (pME18Neo/Flag-Vpr) and pGEX-6P-3 encoding GST-tagged Vpr (pGEX-6P-3/GST-Vpr) have been described previously [57, 58]. The molecular clone vectors pNL4-3-Luc-*env*(−) and pNL4-3-Luc-*env*(−)*vpr*(−) and an expression construct for VSV-G (pVSV-G) were kindly gifted by Dr. Ishizaka (Department of Intractable Diseases, National Center for Global Health and Medicine). For construction of the vector pME18Neo/Flag-Vpr-IRES-ZsGreen1 and the control vector pME18Neo/Flag-IRES-ZsGreen1, a fragment containing an IRES sequence and a ZsGreen1-coding sequence was amplified by polymerase chain reaction (PCR) using the primers 5'-CCCAAACTTAAGCTTGGTACCGA-3' and 5'-TAGCGGCCGCTCAGGGCAAGGCGGAGCCGGAG-3' and pRetroX-IRES-ZsGreen1 (Clontech Laboratories, Mountain View, CA, USA) as a template. The PCR fragment was subcloned into pME18Neo/Flag-Vpr and pME18Neo/Flag at the *Not*I site.

For construction of the expression vector pCAGGS encoding HA-tagged HIP1 (pCAGGS/HA-HIP1), human *HIP1* mRNA was amplified by reverse transcription (RT)-PCR from RNA derived from HeLa cells. RT was performed with an oligo-dT primer, and PCR was performed using the primers 5'-AAAGATATCGGATCGGATGGCCAGCTCCATGAAGCAGGTGCCCAA-3' and 5'-AAAGCGGCCGCCTATTCTTTTTCGGTTACCACTTC-3'. The PCR fragment was subcloned into the pCAGGS/HA vector between the *Eco*RV and *Not*I sites. For construction of the pCAGGS/HA-siR-HIP1 vector, the mutant was generated using standard PCR mutagenesis techniques using pCAGGS/HA-HIP1 as a template.

siRNA

siRNAs against 256 genes were prepared as an siRNA mini-library [59], and those targeting *HIP1* and *DCAF1* were designed using BLOCK-iT RNAi Designer (Invitrogen). The siRNA forward sequences targeting *HIP1* were 5'-CACAGACCUUCUGGUCUGUUGUCAA-3' for siRNA#1 and 5'-GGAGCUAAUGGUGUGUUCUCAUGAA-3' for siRNA#2. The siRNA forward sequence targeting *DCAF1* was 5'-CCCUGGGUGAUUGGCACCAAUUAUA-3'.

Immunoprecipitation

293T cells were co-transfected with the indicated vectors, and at 48-h post-transfection, the cells were lysed with lysis buffer [50 mM Tris–HCl (pH 7.4), 150 mM NaCl, and 0.5% NP-40] supplemented with a

protease-inhibitor cocktail (Roche, Basel, Switzerland) for 30 min on ice. The lysates were centrifuged at 15,000 rpm for 5 min, and the supernatants were collected and mixed with Anti-FLAG M2 agarose beads (Sigma-Aldrich) and incubated at 4°C for 18 h with gentle rotation. The beads were washed five times with lysis buffer, and the bound proteins were eluted using the FLAG peptide (Sigma-Aldrich). Eluted proteins were fractionated by 6% and 15% sodium dodecyl sulfate polyacrylamide gel electrophoresis (SDS-PAGE) and analyzed western blot.

Protein expression and purification

Recombinant GST or GST-Vpr was expressed in *Escherichia coli* BL21 CodonPlus (DE3)-RIL cells (Stratagene, San Diego, CA, USA). Expression was induced with 1 mM isopropyl β-D-1-thiogalactopyranoside at 16°C for 24 h, followed by lysis with BugBuster reagent (Novagen; Merck, Kenilworth, NJ, USA) according to manufacturer instructions. The lysate was cleared by centrifugation, and the soluble fraction was mixed with glutathione-Sepharose 4 FastFlow beads (GE Healthcare, Pittsburgh, PA, USA), which were centrifuged and washed with BugBuster reagent and phosphate-buffered saline (PBS).

To express and purify HA-HIP1, 293T cells were transfected with pCAGGS/HA-HIP1 using FuGene HD transfection reagent (Promega), and at 48-h post-transfection, the cells were collected and lysed with wash buffer. The lysates were centrifuged at 15,000 rpm for 5 min, and the supernatants were collected, mixed with Anti-HA agarose beads (Sigma-Aldrich), and incubated at 4°C for 1 h with gentle rotation. The affinity beads were washed with wash buffer twice, and HA-HIP1 was eluted using the HA peptide (Sigma-Aldrich).

Pull-down assay

Purified HA-HIP1 was incubated with GST or GST-Vpr preadsorbed onto glutathione-Sepharose 4 FastFlow beads at 4°C for 2 h in wash buffer. The beads were then washed with wash buffer five times, and bound proteins were eluted by incubation with sample buffer for SDS-PAGE at 100°C for 5 min. Eluted proteins were fractionated by 6% SDS-PAGE for western blotting.

Western blotting

Cells were lysed for 30 min on ice in 10 mM Tris-HCl (pH 8.0), 150 mM NaCl, 5 mM EDTA, 1% Triton X-100, and 0.1% SDS supplemented with a protease-inhibitor cocktail (Roche). Lysates were mixed with SDS-PAGE sample buffer and boiled for 5 min. Protein concentrations were determined with a BCA protein assay kit (Pierce; Thermo Fisher Scientific, Waltham, MA, USA) using bovine serum albumin as a standard. Equal amounts of total protein were examined by western blotting using the following antibodies: anti-Flag monoclonal antibody (mAb; M2; Sigma-Aldrich), anti-Flag polyclonal Ab (Sigma-Aldrich), anti-β-actin mAb (Sigma-Aldrich), anti-HA mAb (MBL International, Woburn, MA, USA), anti-HIP1 mAb (Novus Biologicals, Littleton, CO, USA), anti-VprBP polyclonal Ab (Proteintech, Rosemont, IL, USA), horseradish-peroxidase (HRP)-conjugated goat anti-mouse IgG (Amersham Biosciences, Little Chalfont,

UK), and HRP-conjugated goat anti-rabbit IgG (Amersham Biosciences). Signals were visualized after treatment with SuperSignal West Pico chemiluminescent substrate (Pierce; Thermo Fisher Scientific).

Analysis of cell cycle profiles by CELAVIEW RS100

HeLa cells were plated in 24-well polystyrene plates. To analyze the effect of siRNA transfection on Vpr-induced G2 arrest, the cells were co-transfected with siRNAs and either pME18Neo/FVpr-IRES-ZsGreen1 or pME18Neo/Flag-IRES-ZsGreen1 and cultured for 48 h. To analyze the effect of *HIP1* overexpression on the inhibition of Vpr-induced G2 arrest following *HIP1* knockdown, the cells were co-transfected with siRNAs, pME18Neo/FVpr-IRES-ZsGreen1, and pCAGGS/HA-siR-HIP1 or pCAGGS/HA and cultured for 48 h. To analyze the effect of *HIP1* knockdown on etoposide-induced G2 arrest, the cells were transfected with siRNAs. At 24-h post-transfection, the cells were treated with 10 μM etoposide and cultured for 24 h. These cells were fixed and stained with 3.6% formaldehyde containing 5 μg/ml Hoechst33342 for 10 min at room temperature and then washed three times with PBS. For each sample, at least 200 ZsGreen1-positive cells were observed and analyzed using a CELAVIEW microscope (RS100; Olympus, Tokyo, Japan).

Analysis of cell cycle profiles by flow cytometry

HeLa cells were co-transfected with siRNAs and either pME18Neo/Flag-Vpr-IRES-ZsGreen1 or pME18Neo/Flag-IRES-ZsGreen1 as a control and cultured for 48 h. The cells were harvested and fixed with 1% formaldehyde, followed by 70% ethanol. Fixed cells were incubated in PBS containing RNase A (50 μg/ml) at 37°C for 20 min and then stained with propidium iodide (40 μg/ml). For each sample, at least 7,000 cells were analyzed using a FACS Calibur instrument (Becton Dickinson, Franklin Lakes, NJ, USA) with CELL Quest software (Becton Dickinson). Ratios of the numbers of cells in G1 and G2/M phases (G2/M:G1 ratios) were calculated using ModFit LT software (Verity Software House, Topsham, ME, USA).

Viral stock and viral infection of macrophages

To generate viral stocks, 293T cells were co-transfected with pNL4-3-Luc-*env*(−) or pNL4-3-Luc-*env*(−)*vpr*(−) and pVSV-G using FuGENE HD (Promega), and the virus was harvested at 48-h post-transfection. HIV-1 titers were measured using an anti-p24 enzyme-linked immunosorbent assay kit (Ryukyu Immunology, Okinawa, Japan).

Primary macrophages in 24-well plates were inoculated with VSV-G pseudotyped reporter viruses [NL-Luc-E^-R^+ (VSV-G) or NL-Luc-E^-R^- (VSV-G); 4 ng of p24 antigen], cultured for 6 days, harvested, and lysed in luciferase assay substrate (Promega). Infectivity was determined by measurement of luciferase activity.

Statistical analysis

Statistical analyses were performed by Prism 8.0 (GraphPad software, San Diego, CA, USA). For two-group comparisons, two-tailed Student's *t*-test was used. Data are presented as mean ± SD and were

considered statistically significant when the *P* value was <0.05.

List Of Abbreviations

HIV-1
human immunodeficiency virus type 1
DDB1
DNA damage-binding protein 1
CUL4
Cullin4
DCAF1
DDB1- and CUL4-associated factor 1
SLX4
synthetic lethal of unknown (X) function 4
LTR
long terminal repeat
ATR
ataxia telangiectasia-mutated and Rad3-related protein
HIP1
Huntingtin-interacting protein 1
siRNA
small-interfering RNA
IRES
internal ribosomal entry site
WT
wild-type
GST
glutathione-S-transferase
γ-H2AX
phosphorylated histone 2A variant X
PBMCs
peripheral blood mononuclear cells
VSV-G
vesicular stomatitis virus G protein
PP2A
protein phosphatase 2
FCS
fetal calf serum
M-CSF
macrophage colony-stimulating factor

PCR
polymerase chain reaction
RT
reverse transcription
mAb
monoclonal antibody
HRP
horseradish-peroxidase

Declarations

Ethics approval and consent to participate

All participants provided written informed consent. Ethics approval for this study was granted by the RIKEN Ethics Committees [Certificate No. Wako 24–7] and by the Nihon University School of Medicine Ethics Committees [Certificate No. 22-7-10].

Consent for publication

Not applicable

Availability of data and materials

The datasets used and/or analyzed during the current study are available from the corresponding author on reasonable request.

Competing interests

The authors declare that they have no competing interests.

Funding

This study was partially supported by a grant (Research on HIV/AIDS project no. H22-003) from the Ministry of Health, Labor, and Welfare of Japan, and by a grant (Research on HIV/AIDS projects no. 16fk0410104j0001) from the Japan Agency for Medical Research and Development.

Authors' contributions

Conceived and designed the experiments: YA and TM. Performed the experiments: TM and CN. Analyzed the data: TM and YA. Contributed reagents/materials/analysis tools: YA. Wrote the paper: TM and YA. All authors read and approved the final manuscript.

Acknowledgments

We thank Dr. Naoki Yamamoto of National University of Singapore, Dr. Hironori Sato of National Institute of Infectious Diseases, and Dr. Jun Komano of Osaka Prefectural Institute of Public Health for kindly providing of siRNA library. We are grateful to the RIKEN BSI-Olympus Collaboration Center for imaging equipment and software, and RIKEN BSI Research Resources Center for help with sequence analysis. We would like to thank Editage (www.editage.com) for English language editing.

References

1. Hashizume C, et al. Human immunodeficiency virus type 1 Vpr interacts with spliceosomal protein SAP145 to mediate cellular pre-mRNA splicing inhibition. Microbes Infect. 2007;9(4):490–7.
2. Kuramitsu M, et al. A novel role for Vpr of human immunodeficiency virus type 1 as a regulator of the splicing of cellular pre-mRNA. Microbes Infect. 2005;7(9–10):1150–60.
3. Zhang X, Aida Y. HIV-1 Vpr: a novel role in regulating RNA splicing. Curr HIV Res. 2009;7(2):163–8.
4. Chutiwitoonchai N, et al. HIV-1 Vpr Abrogates the Effect of TSG101 Overexpression to Support Virus Release. PLoS One. 2016;11(9):e0163100.
5. Kamata M, et al. Importin-alpha promotes passage through the nuclear pore complex of human immunodeficiency virus type 1 Vpr. J Virol. 2005;79(6):3557–64.
6. Nitahara-Kasahara Y, et al. Novel nuclear import of Vpr promoted by importin alpha is crucial for human immunodeficiency virus type 1 replication in macrophages. J Virol. 2007;81(10):5284–93.
7. Popov S, et al. Viral protein R regulates nuclear import of the HIV-1 pre-integration complex. EMBO J. 1998;17(4):909–17.
8. Mashiba M, et al. Vpr overcomes macrophage-specific restriction of HIV-1 Env expression and virion production. Cell Host Microbe. 2014;16(6):722–35.
9. Zhang X, et al. HIV-1 Vpr increases Env expression by preventing Env from endoplasmic reticulum-associated protein degradation (ERAD). Virology. 2016;496:194–202.
10. Wang Q, Su L. *Vpr Enhances HIV-1 Env Processing and Virion Infectivity in Macrophages by Modulating TET2-Dependent IFITM3 Expression*. MBio, 2019. 10(4).
11. Lv L, et al., Vpr Targets TET2 for Degradation by CRL4(VprBP) E3 Ligase to Sustain IL-6 Expression and Enhance HIV-1 Replication. Mol Cell, 2018. 70(5): 961–70 e5.
12. Hrecka K, et al. HIV-1 and HIV-2 exhibit divergent interactions with HLTF and UNG2 DNA repair proteins. Proc Natl Acad Sci U S A. 2016;113(27):E3921-30.
13. Lahouassa H, et al. HIV-1 Vpr degrades the HLTF DNA translocase in T cells and macrophages. Proc Natl Acad Sci U S A. 2016;113(19):5311–6.
14. Yan J, et al., *HIV-1 Vpr Reprograms CLR4(DCAF1) E3 Ubiquitin Ligase to Antagonize Exonuclease 1-Mediated Restriction of HIV-1 Infection*. MBio, 2018. 9(5).
15. Yan J, et al. HIV-1 Vpr counteracts HLTF-mediated restriction of HIV-1 infection in T cells. Proc Natl Acad Sci U S A. 2019;116(19):9568–77.

16. Ayyavoo V, et al. HIV-1 Vpr suppresses immune activation and apoptosis through regulation of nuclear factor kappa B. Nat Med. 1997;3(10):1117–23.
17. Jowett JB, et al. The human immunodeficiency virus type 1 vpr gene arrests infected T cells in the G2 + M phase of the cell cycle. J Virol. 1995;69(10):6304–13.
18. Murakami T, Aida Y. Visualizing Vpr-induced G2 arrest and apoptosis. PLoS One. 2014;9(1):e86840.
19. Nishizawa M, et al. Induction of apoptosis by the Vpr protein of human immunodeficiency virus type 1 occurs independently of G(2) arrest of the cell cycle. Virology. 2000;276(1):16–26.
20. Nonaka M, et al. The human immunodeficiency virus type 1 Vpr protein and its carboxy-terminally truncated form induce apoptosis in tumor cells. Cancer Cell Int. 2009;9:20.
21. Rogel ME, Wu LI, Emerman M. The human immunodeficiency virus type 1 vpr gene prevents cell proliferation during chronic infection. J Virol. 1995;69(2):882–8.
22. Chang H, et al., *Distinct MCM10 Proteasomal Degradation Profiles by Primate Lentiviruses Vpr Proteins*. Viruses, 2020. 12(1).
23. Hrecka K, et al. Lentiviral Vpr usurps Cul4-DDB1[VprBP] E3 ubiquitin ligase to modulate cell cycle. Proc Natl Acad Sci U S A. 2007;104(28):11778–83.
24. Laguette N, et al. Premature activation of the SLX4 complex by Vpr promotes G2/M arrest and escape from innate immune sensing. Cell. 2014;156(1–2):134–45.
25. Miyatake H, et al. Molecular Mechanism of HIV-1 Vpr for Binding to Importin-alpha. J Mol Biol. 2016;428(13):2744–57.
26. Murakami H, et al., *Protein Arginine N-methyltransferases 5 and 7 Promote HIV-1 Production*. Viruses, 2020. 12(3).
27. Felzien LK, et al. HIV transcriptional activation by the accessory protein, VPR, is mediated by the p300 co-activator. Proc Natl Acad Sci U S A. 1998;95(9):5281–6.
28. Goh WC, et al. HIV-1 Vpr increases viral expression by manipulation of the cell cycle: a mechanism for selection of Vpr in vivo. Nat Med. 1998;4(1):65–71.
29. Planelles V, et al. Vpr-induced cell cycle arrest is conserved among primate lentiviruses. J Virol. 1996;70(4):2516–24.
30. Stivahtis GL, et al. Conservation and host specificity of Vpr-mediated cell cycle arrest suggest a fundamental role in primate lentivirus evolution and biology. J Virol. 1997;71(6):4331–8.
31. Sato K, et al. HIV-1 Vpr accelerates viral replication during acute infection by exploitation of proliferating CD4 + T cells in vivo. PLoS Pathog. 2013;9(12):e1003812.
32. Poon B, et al. Human immunodeficiency virus type 1 vpr gene induces phenotypic effects similar to those of the DNA alkylating agent, nitrogen mustard. J Virol. 1997;71(5):3961–71.
33. Zimmerman ES, et al. Human immunodeficiency virus type 1 Vpr-mediated G2 arrest requires Rad17 and Hus1 and induces nuclear BRCA1 and gamma-H2AX focus formation. Mol Cell Biol. 2004;24(21):9286–94.

34. Zimmerman ES, et al. Human immunodeficiency virus type 1 Vpr induces DNA replication stress in vitro and in vivo. J Virol. 2006;80(21):10407–18.
35. Belzile JP, et al. HIV-1 Vpr-mediated G2 arrest involves the DDB1-CUL4AVPRBP E3 ubiquitin ligase. PLoS Pathog. 2007;3(7):e85.
36. DeHart JL, et al. HIV-1 Vpr activates the G2 checkpoint through manipulation of the ubiquitin proteasome system. Virol J. 2007;4:57.
37. Le Rouzic E, et al. HIV1 Vpr arrests the cell cycle by recruiting DCAF1/VprBP, a receptor of the Cul4-DDB1 ubiquitin ligase. Cell Cycle. 2007;6(2):182–8.
38. Schrofelbauer B, Hakata Y, Landau NR. HIV-1 Vpr function is mediated by interaction with the damage-specific DNA-binding protein DDB1. Proc Natl Acad Sci U S A. 2007;104(10):4130–5.
39. Wen X, et al. The HIV1 protein Vpr acts to promote G2 cell cycle arrest by engaging a DDB1 and Cullin4A-containing ubiquitin ligase complex using VprBP/DCAF1 as an adaptor. J Biol Chem. 2007;282(37):27046–57.
40. Berger G, et al. G2/M cell cycle arrest correlates with primate lentiviral Vpr interaction with the SLX4 complex. J Virol. 2015;89(1):230–40.
41. Fregoso OI, Emerman M. *Activation of the DNA Damage Response Is a Conserved Function of HIV-1 and HIV-2 Vpr That Is Independent of SLX4 Recruitment*. MBio, 2016. 7(5).
42. Orenstein JM, Fox C, Wahl SM. Macrophages as a source of HIV during opportunistic infections. Science. 1997;276(5320):1857–61.
43. Sattentau QJ, Stevenson M. Macrophages and HIV-1: An Unhealthy Constellation. Cell Host Microbe. 2016;19(3):304–10.
44. Subbramanian RA, et al. Human immunodeficiency virus type 1 Vpr is a positive regulator of viral transcription and infectivity in primary human macrophages. J Exp Med. 1998;187(7):1103–11.
45. Kalchman MA, et al. HIP1, a human homologue of S. cerevisiae Sla2p, interacts with membrane-associated huntingtin in the brain. Nat Genet. 1997;16(1):44–53.
46. Wedemeyer N, et al., *Localization of the human HIP1 gene close to the elastin (ELN) locus on 7q11.23.* Genomics, 1997. **46**(2): p. 313-5.
47. Metzler M, et al. HIP1 functions in clathrin-mediated endocytosis through binding to clathrin and adaptor protein 2. J Biol Chem. 2001;276(42):39271–6.
48. Mishra SK, et al. Clathrin- and AP-2-binding sites in HIP1 uncover a general assembly role for endocytic accessory proteins. J Biol Chem. 2001;276(49):46230–6.
49. Waelter S, et al. The huntingtin interacting protein HIP1 is a clathrin and alpha-adaptin-binding protein involved in receptor-mediated endocytosis. Hum Mol Genet. 2001;10(17):1807–17.
50. Rao DS, et al. Altered receptor trafficking in Huntingtin Interacting Protein 1-transformed cells. Cancer Cell. 2003;3(5):471–82.
51. Rao DS, et al. Huntingtin-interacting protein 1 is overexpressed in prostate and colon cancer and is critical for cellular survival. J Clin Invest. 2002;110(3):351–60.

52. Choi SA, Kim SJ, Chung KC. Huntingtin-interacting protein 1-mediated neuronal cell death occurs through intrinsic apoptotic pathways and mitochondrial alterations. FEBS Lett. 2006;580(22):5275–82.
53. Kang JE, et al. Regulation of the proapoptotic activity of huntingtin interacting protein 1 by Dyrk1 and caspase-3 in hippocampal neuroprogenitor cells. J Neurosci Res. 2005;81(1):62–72.
54. Belzile JP, et al. Formation of mobile chromatin-associated nuclear foci containing HIV-1 Vpr and VPRBP is critical for the induction of G2 cell cycle arrest. PLoS Pathog. 2010;6(9):e1001080.
55. Belzile JP, et al. HIV-1 Vpr induces the K48-linked polyubiquitination and proteasomal degradation of target cellular proteins to activate ATR and promote G2 arrest. J Virol. 2010;84(7):3320–30.
56. Li G, et al. Phosphatase type 2A-dependent and -independent pathways for ATR phosphorylation of Chk1. J Biol Chem. 2007;282(10):7287–98.
57. Nishino Y, et al. Human immunodeficiency virus type 1 Vpr gene product prevents cell proliferation on mouse NIH3T3 cells without the G2 arrest of the cell cycle. Biochem Biophys Res Commun. 1997;232(2):550–4.
58. Takeda E, et al. Nuclear exportin receptor CAS regulates the NPI-1-mediated nuclear import of HIV-1 Vpr. PLoS One. 2011;6(11):e27815.
59. Kameoka M, et al. Identification of the suppressive factors for human immunodeficiency virus type-1 replication using the siRNA mini-library directed against host cellular genes. Biochem Biophys Res Commun. 2007;359(3):729–34.

Figures

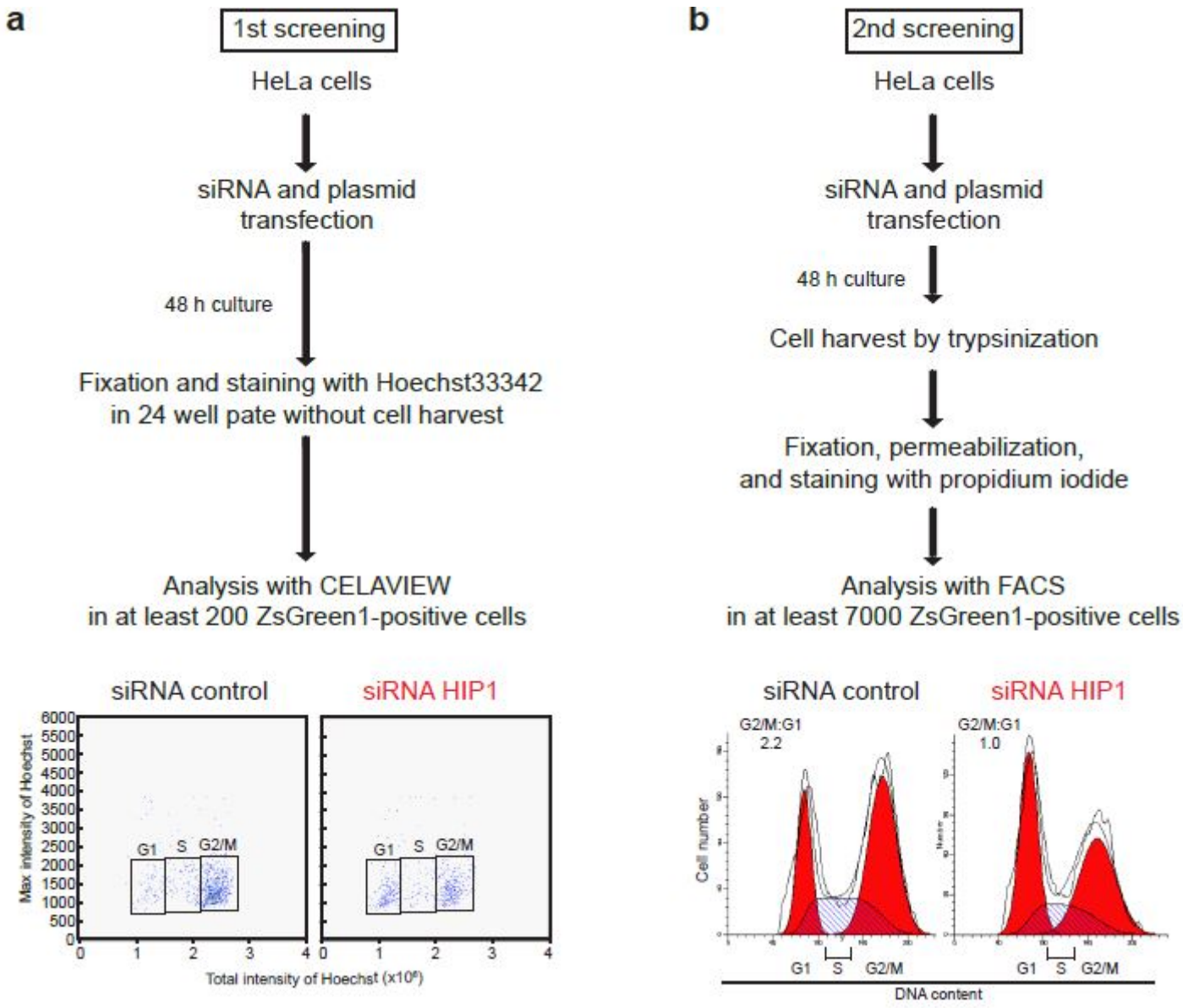

Figure 1

Summary of siRNA screening for candidate suppressors of Vpr-induced G2 arrest. (A) For the initial screening, HeLa cells were co-transfected with pME18Neo/Flag-Vpr-IRES-ZsGreen1 and 100 nM individual siRNAs from the siRNA mini-library or control siRNA. At 48-h post-transfection, cells were fixed and stained with 5 μg/ml Hoechst33342 to measure DNA content in at least 200 ZsGreen1+ cells using CELAVIEW RS100. (B) For secondary screening, HeLa cells were co-transfected with pME18Neo/Flag-Vpr-IRES-ZsGreen1 and control siRNA or 100 nM of individual siRNAs that inhibited Vpr-induced G2 arrest according to the initial screen. At 48-h post-transfection, cells were harvested by trypsinization, fixed, permeabilized, treated with RNase A, and stained with 50 μg/ml propidium iodide to measure DNA content in at least 7,000 ZsGreen1+ cells by flow cytometry.

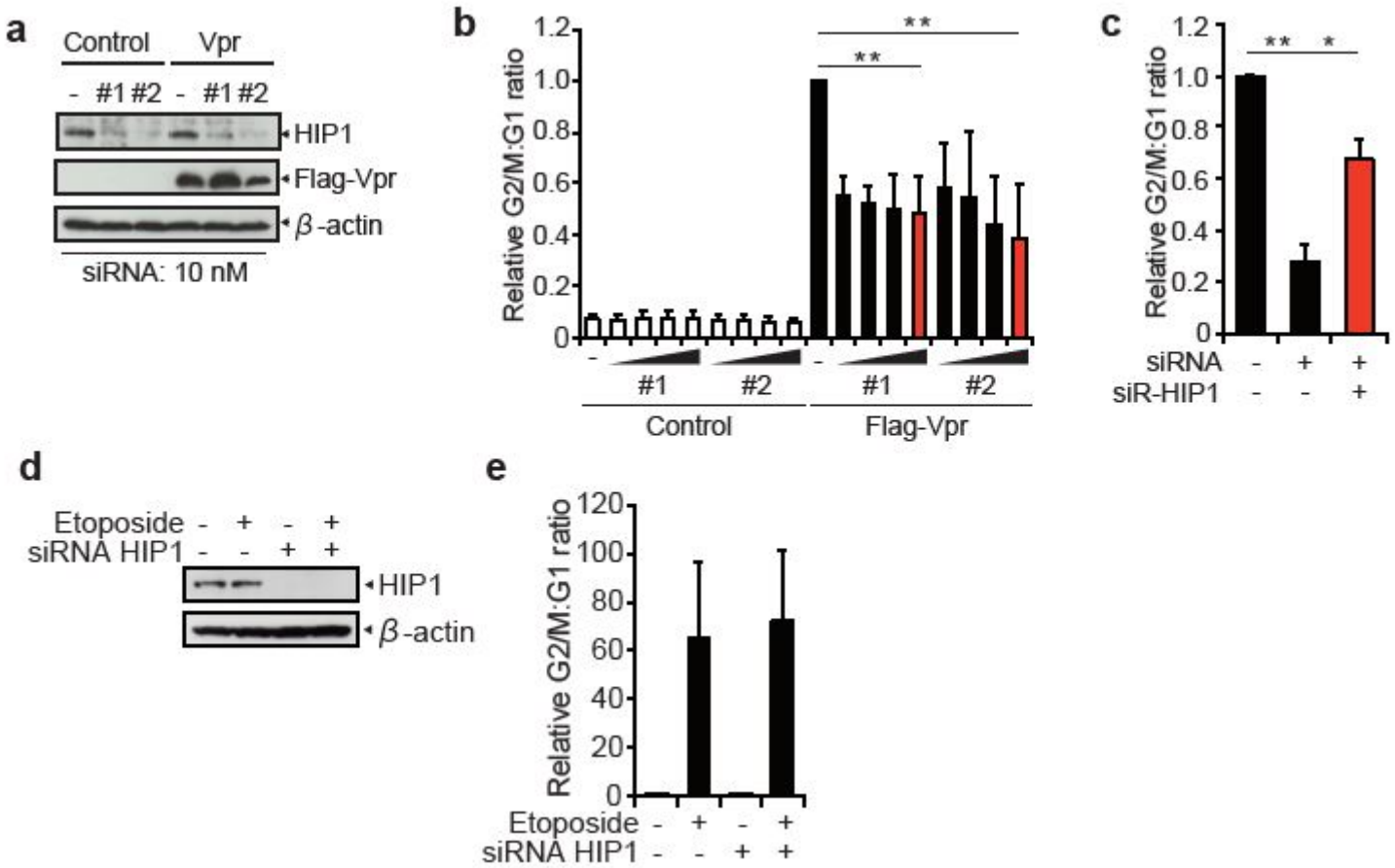

Figure 2

HIP1 specifically enhances Vpr-induced G2 arrest. (A and B) HeLa cells were co-transfected with pME18Neo/Flag-Vpr-IRES-ZsGreen1 or control pME18Neo/Flag-IRES-ZsGreen1 and either 10 nM HIP1 (siRNA #1 and #2) or control siRNA (A) and either HIP1 (siRNA #1 and #2; 1, 2.5, 5, or 10 nM) or control siRNA, respectively (B), and cultured for 48 h. (A) Cells were lysed and subjected to 6% and 15% SDS-PAGE and western blot using an anti-HIP1 mAb, anti-Flag M2 mAb, and anti-β-actin mAb. (B) Cells were fixed and stained with 5 μg/ml Hoechst33342 to measure DNA content in ZsGreen1+ cells using CELAVIEW RS100. The relative G2/M:G1 ratio was plotted, and data represent the mean ± SD of three independent experiments. (C) HeLa cells were co-transfected with pME18Neo/Flag-Vpr-IRES-ZsGreen1 and pCAGGS/HA-siR-HIP1 (carrying synonymous nucleotide mutations at the third codon of the siRNA-targeting site) or control pCAGGS/HA and either 10 nM HIP1 (siRNA #2) or control siRNA. At 48-h post-transfection, cells were fixed, permeabilized, stained with the anti-HA mAb, and then with Alexa Fluor 594-conjugated secondary Ab and Hoechst33342. The DNA content of ZsGreen1+ and Alexa Fluor 594+ cells was analyzed by CELAVIEW RS100. The relative G2/M:G1 ratio was plotted, and data represent the mean ± SD of three independent experiments. (D and E) HeLa cells were transfected with either 10 nM HIP1 (siRNA #2) or control siRNA and cultured for 24 h. Cells were treated with 10 μM etoposide and cultured for 24 h. Cells were lysed and subjected to SDS-PAGE and western blot using anti-HIP1 and anti-β-actin mAbs (D) or fixed and stained with Hoechst33342 (E). The DNA content of cells was analyzed by

CELAVIEW RS100. The relative G2/M:G1 ratio is plotted, and data represent the mean ± SD of triplicate wells. *p < 0.05, **p < 0.01 via two-tailed Student's t test.

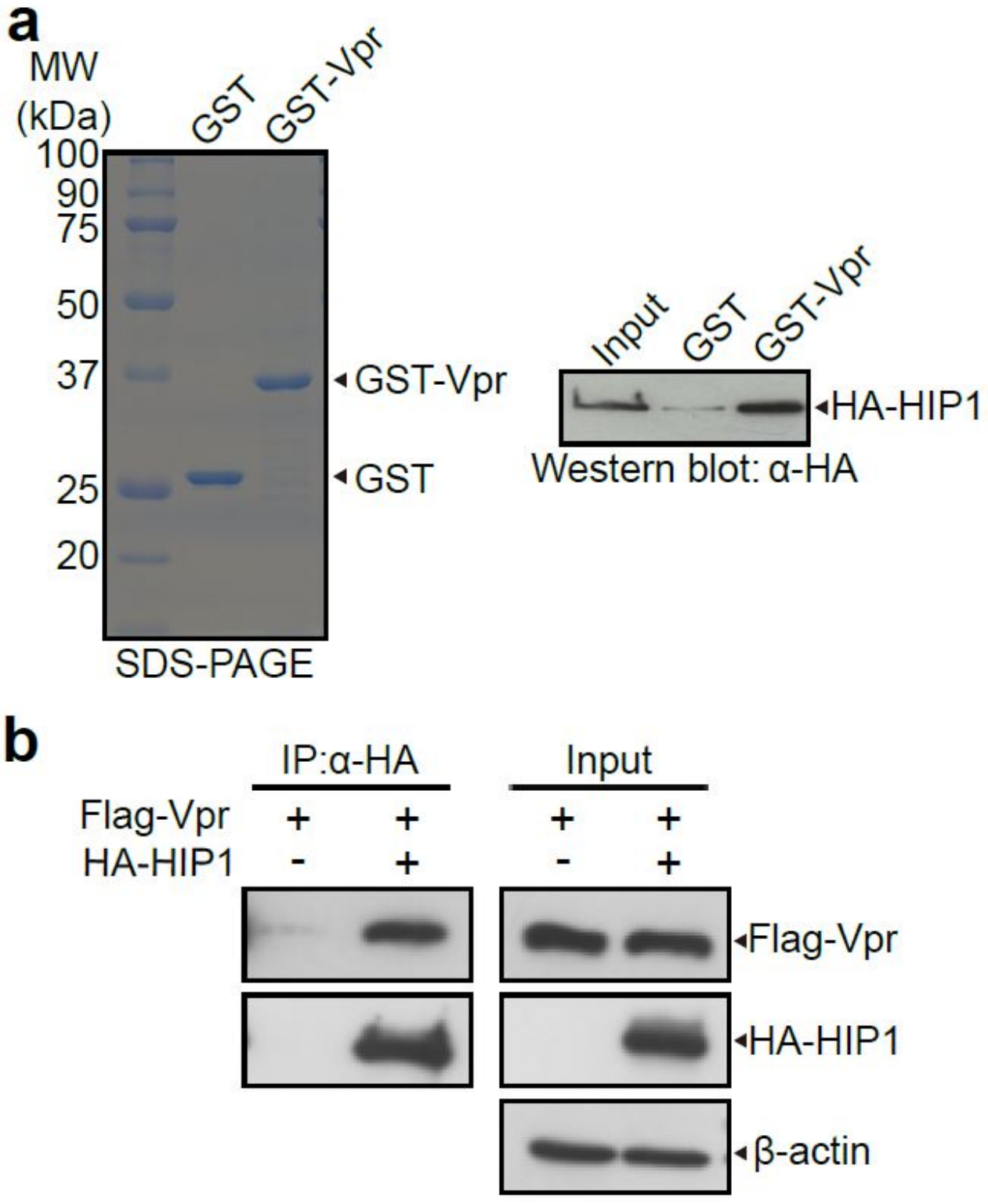

Figure 3

Vpr directly interacts with HIP1. (A) GST and GST-Vpr were resolved by 12% SDS-PAGE and stained with Coomassie Brilliant Blue (CBB) (left). Glutathione-Sepharose beads mixed with the GST-Vpr or GST alone were incubated with purified HA-HIP1 protein. The bound fractions and 10% of the input were analyzed by

western blot using the anti-HA mAb (right). The positions of HIP1, GST-Vpr, and GST are indicated. (B) 293T cells were co-transfected with pME18Neo/Flag-Vpr or control pME18Neo and pCAGGS/HA-HIP1. At 48-h post-transfection, cells were lysed, and the lysates were subjected to immunoprecipitation assays using anti-FLAG M2 agarose and the FLAG peptide. The bound fractions and inputs were analyzed by western blotting using the anti-HA mAb, anti-Flag polyclonal Ab, and anti-β-actin mAb.

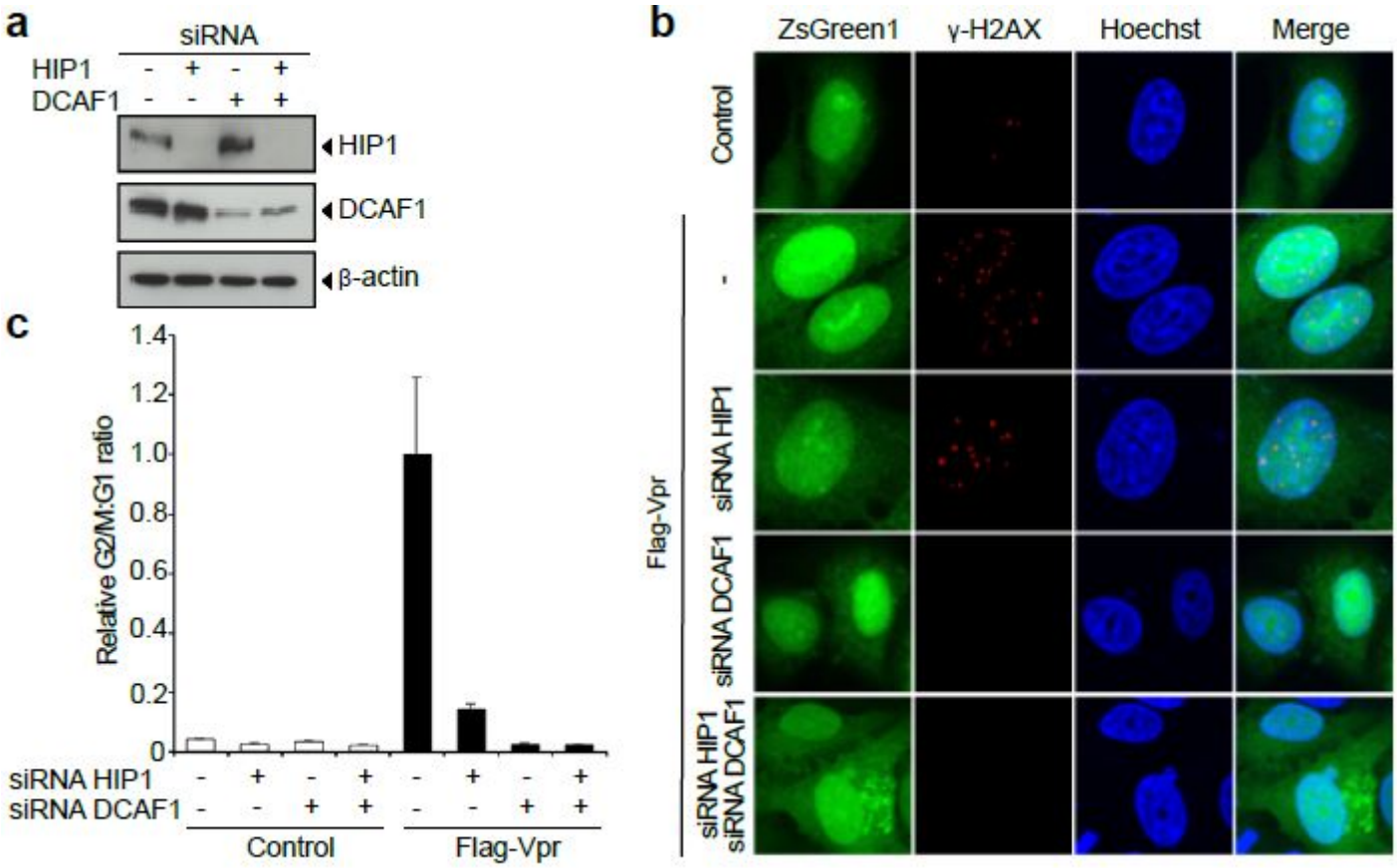

Figure 4

Vpr induces DNA double-strand breaks in HIP1-knockdown cells. (A) HeLa cells were transfected with 5 nM HIP1 (siRNA #2), DCAF1, or a combination of 5 nM HIP1 (siRNA #2) and 5 nM DCAF1 siRNAs. The total amount of siRNA was adjusted to 10 nM with control siRNA. At 48-h post-transfection, cells were lysed and subjected to SDS-PAGE and western blot using the anti-HIP1 mAb, anti-DCAF1 mAb, and anti-β-actin mAb. The positions of HIP1, Flag-Vpr, and β-actin are indicated. (B and C) HeLa cells were co-transfected with pME/Flag-Vpr-IRES-ZsGreen1 or control pME/Flag-IRES-ZsGreen1 and 5 nM HIP1 (siRNA #2), DCAF1, or a combination of 5 nM HIP1 (siRNA #2) and/or 5 nM DCAF1 siRNAs. The total amount of siRNA was adjusted to 10 nM with control siRNA. (B) At 48-h post-transfection, cells were fixed, permeabilized, and stained with the anti-γ-H2AX mAb, followed by Alexa Fluor 594-conjugated secondary antibody and 5 μg/ml Hoechst33342. Cells were analyzed by a confocal microscopy. Cells showing green fluorescence (ZsGreen1+) and red foci indicated the presence of DNA double-strand breaks, and blue fluorescence indicated nuclei. (C) At 48 h post-transfection, cells were fixed and stained with 5 μg/ml Hoechst33342 to measure DNA content in ZsGreen1+ cells, which were analyzed by CELAVIEW RS100. The relative G2/M:G1 ratio was plotted, and data represent the mean ± SD of triplicate wells.

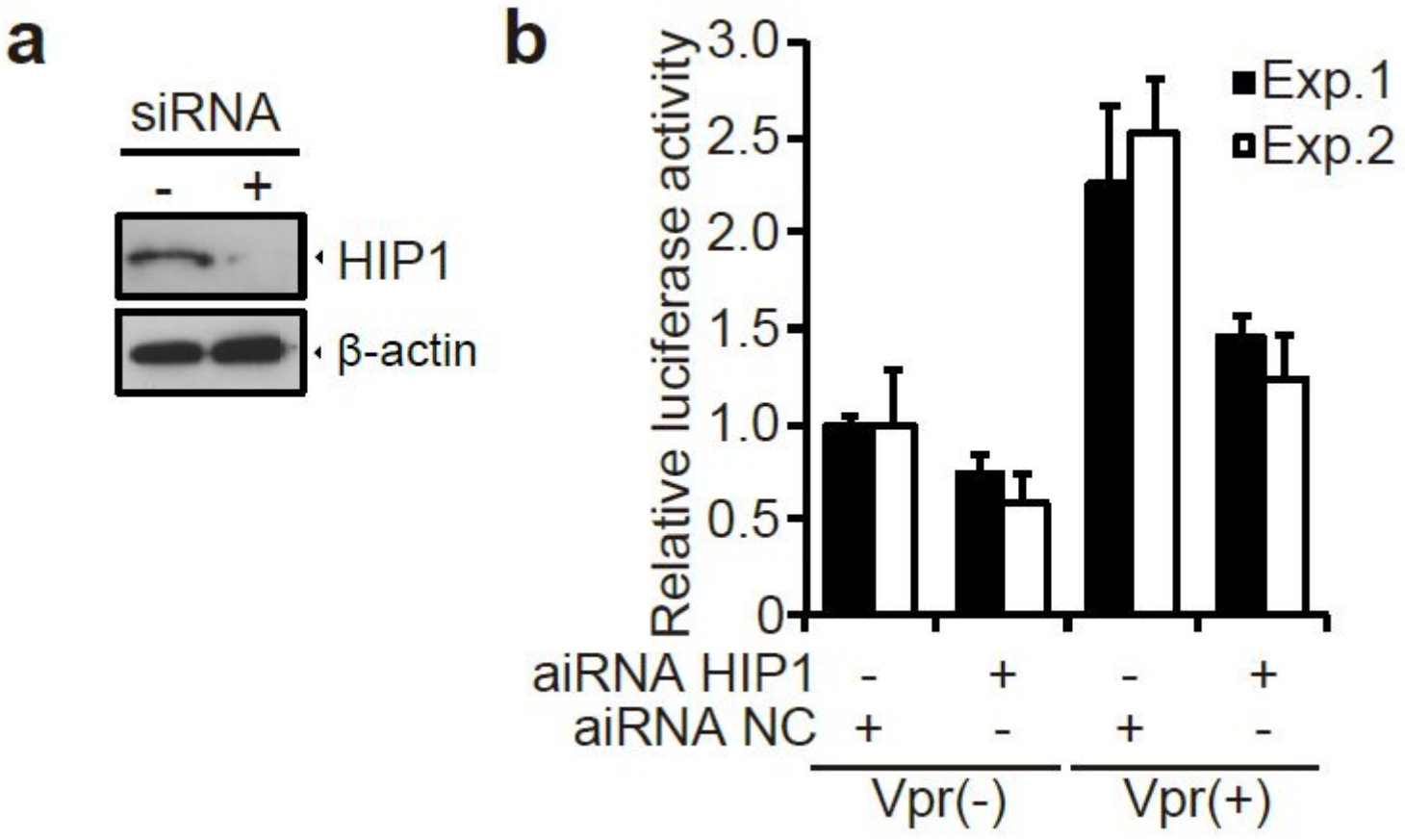

Figure 5

HIP1 enhances HIV-1 infection in macrophages in a Vpr-dependent manner. Monocytes isolated from PBMCs of human healthy donor were subsequently differentiated into macrophages by addition of M-CSF, followed by their transfection with 50 nM HIP1 (siRNA #2) and control siRNA. (A) At 48-h post-transfection, cells were lysed and subjected to 6% SDS-PAGE and western blotting using the anti-HIP1 mAb and anti-β-actin mAb. The positions of HIP1 and β-actin are indicated. (B) At 24-h post-transfection, cells were infected with 4 ng p24 VSV-G-pseudotyped-HIV-1 or -HIV-1 ΔVpr. At 6-days post-infection, cells were lysed, and infectivity was determined by measuring luciferase activity. Data represent the mean ± SD of triplicate wells.